

Supporting Information

δ -Carboline-based Bipolar Host Materials for Deep Blue Thermally Activated Delayed Fluorescence OLEDs with High Efficiency and Low Roll-off Characteristic

Ji Su Moon, Dae Hyun Ahn, Si Woo Kim, Seung Yeon Lee, Ju Young Lee*, and Jang Hyuk Kwon*

Department of Information Display, Kyung Hee University, 26 Kyungheedaero, Dongdaemoongu, Seoul, 130-701, Republic of Korea.

* juyoung105@khu.ac.kr (Ju young Lee); jhkwon@khu.ac.kr (Jang Hyuk Kwon)

Table of Contents

1. Experimental section

1.1. Synthesis of materials

1.2. Computational data

1.3. Material characterization

1.4. Device fabrication and measurement

2. T_g , T_m , and T_d of synthesized materials from DSC and TGA measurement

3. Results of Cyclic Voltammetry.

4. Prompt and delayed PL spectra of DMAC-DPS in each host materials.

5. NMR data

1. EXPERIMENTAL SECTION

1.1 Synthesis.

CzCbPy

A mixture of 8-bromo-5H-pyrido[3,2-b]indole (9.4 g, 38.0 mmol), 2-bromopyridine (5.0 g, 31.6 mmol), trans-1,2-diaminocyclohexane (2.2 g, 19.0 mmol), copper(I) iodide (1.8 g, 9.5 mmol), and potassium phosphate tribasic (13.4 g, 63.2 mmol) in nitrobenzene (150 mL) was refluxed for 6h under nitrogen atmosphere. The reaction mixture was cooled to room temperature, extracted with ethyl acetate and distilled water. The organic layer was dried over anhydrous magnesium sulfate and evaporated in vacuo to give the crude product, which was purified by column chromatography on silica gel to provide 8-bromo-5-(pyridin-2-yl)-5H-pyrido[3,2-b]indole (7.7 g, 75%). The titled compound was obtained as a white solid (4.8 g, 51 %) by using a similar procedure for the above compound with 8-bromo-5-(pyridin-2-yl)-5H-pyrido[3,2-b]indole (7.4 g, 22.8 mmol) and 9H-carbazole (4.6 g, 27.4 mmol) instead of 2-bromopyridine and 8-bromo-5H-pyrido[3,2-b]indole. ¹H NMR (CDCl₃, 400 MHz): δ [ppm] 8.86 (m, 1H), 8.66 (m, 2H), 8.24 (t, J = 8.0 Hz, 1H), 8.17 (d, J = 7.6 Hz, 2H), 8.08 (d, J = 8.4 Hz, 1H), 8.01 (d, J = 8.4 Hz, 2H), 7.76 (d, J = 7.6 Hz, 1H), 7.71 (m, 2H), 7.55 (m, 1H), 7.43-7.49 (m, 3H), 7.38 (t, J = 7.2 Hz, 2H). ¹³C NMR (CDCl₃, 100 MHz): δ [ppm] 151.6, 150.6, 142.2, 141.0, 140.8, 140.0, 139.3, 133.6, 129.0, 126.5, 124.7, 122.8, 122.5, 121.7, 121.5, 121.1, 120.8, 120.2, 120.0, 115.3, 114.2, 111.9, 111.8(6). HRMS *m/z* [M]⁺ calcd for C₂₈H₁₈N₄ (M) 410.1531, found: 410.1531.

2CzCbPy

A mixture of 8-bromo-5H-pyrido[3,2-b]indole (7.3 g, 29.7 mmol), 9-(6-bromopyridin-2-yl)-9H-carbazole (8.0 g, 24.8 mmol), trans-1,2-diaminocyclohexane (1.7 g, 14.5 mmol), copper(I) iodide (1.4 g, 7.4 mmol), and potassium phosphate tribasic (10.5 g, 49.6 mmol) in nitrobenzene (120 mL) was refluxed for 6h under nitrogen atmosphere. The reaction mixture was cooled to room temperature, extracted with ethyl acetate and distilled water. The organic layer was dried over anhydrous magnesium sulfate and evaporated in vacuo to give the crude product, which was purified by column chromatography on silica gel to provide 5-(6-(9H-carbazol-9-yl)pyridin-2-yl)-8-bromo-5H-pyrido[3,2-b]indole (7.5 g, 62%). The titled compound was obtained as a white solid (3.5 g, 43 %) by using a similar procedure for the above compound with 5-(6-(9H-carbazol-9-yl)pyridin-2-yl)-8-bromo-5H-pyrido[3,2-b]indole (7.0 g, 14.3 mmol) and 9H-carbazole (2.9 g, 17.1 mmol) instead of 9-(6-bromopyridin-2-yl)-9H-carbazole and 8-bromo-5H-pyrido[3,2-b]indole. ¹H NMR (CDCl₃, 400 MHz): δ [ppm] 9.01 (m, 1H), 8.68 (m, 2H), 8.29 (m, 2H), 8.19 (m, 4H), 8.05 (d, J = 8.0 Hz, 2H), 7.82 (m, 2H), 7.76 (d, J = 8.0 Hz, 1H), 7.38-7.54 (m, 9H), 7.33 (t, J = 7.2 Hz, 2H). ¹³C NMR (CDCl₃, 100 MHz): δ [ppm] 151.9, 150.1, 141.3, 131.1, 139.3, 138.9, 132.6, 126.5, 126.1, 124.7, 123.4, 121.7, 121.4, 120.5, 120.4, 120.3, 120.0, 115.9, 114.3, 113.4, 111.8, 109.8. HRMS *m/z* [M]⁺ calcd for C₄₀H₂₅N₅ (M⁺H) 575.2110, found: 575.2111.

1.2 Computational data. To predict the molecular orbitals and energy levels of new materials, density functional theory (DFT/B3LYP) and time dependent density functional theory (TD-DFT/GGA) simulation were performed with the double numerical plus *d*-functions (DND) atomic orbital basis set. In addition, to determine the molecular packing structures, the simulation was also performed using a polymorph module for each molecule. The molecular simulation were executed with DMol3 module in Material studio 8.0 software package (Accelrys Inc, San Diego, California, United States.).

1.3 Material characterization. ¹H and ¹³C NMR spectra were recorded using Bruker Avance 400 NMR spectrometer. The DSC was performed using a Mettler DSC 821e instrument and the TGA was measured using a Mettler TGA Q50 thermal analysis system using a heating rate of 10 °C/min. High resolution mass were quantified using JMS-7000 (JEOL) at The Central Laboratory for Instrumental Analysis of Kyung Hee University. UV-vis absorption and photoluminescence (PL) spectra were measured using SCINCO S-4100 spectrometer and JASCO FP8500 spectrometer, respectively. The transient PL decay of thin film was recorded using a Quantaaurus-Tau fluorescence lifetime measurement system (C11367-03, Hamamatsu Photonics Co.) in N₂ filled atmosphere. Electrochemical analyses of the synthesized host materials were measured using cyclic voltammetry (CV). CV was performed using EC epsilon electrochemical analysis equipment. To measure the oxidation potential (HOMO) of these host materials, carbon wire, platinum wire and Ag wire in 0.01 M AgNO₃, were used as working , counter and reference electrodes, respectively. The acetonitrile solution containing 0.1M tetrabutyl ammonium perchlorate was used as a supporting electrolyte. Using an internal residual ferrocene/ferrocenium (Fc/Fc⁺) standard, the potential values were converted to the saturated

calomel electrode (SCE) scale. The optical band-gap was determined by using the edge of absorption spectra. The LUMO level of each material was calculated from the optical band gap and HOMO value.

1.4 Device Fabrication and Measurement. To fabricate TADF OLED devices, Indium-Tin-Oxide (ITO) coated glass substrates were cleaned in several steps. First, they were washed in ultrasonic bath with acetone and isopropyl alcohol. After washing, nitrogen was used to dry the substrates and to remove residual solvents followed by UV-ozone treatment for 10 minutes. All organic layers and metal cathode were deposited on pre-cleaned ITO substrates in vacuum evaporation system under vacuum pressure of $\sim 1 \times 10^{-7}$ Torr. The deposition rate of all organic layers was about 0.5 Å/s and the deposition rate of LiF and Al were maintained at 0.1 Å/s and 4 Å/s, respectively. After the deposition process, all devices were encapsulated using glass cover and UV curable resin inside the nitrogen glove box. The emission area was 4 mm² for all the samples studied in this work. The current density versus voltage (J-V) and luminance versus voltage (L-V) characteristics of fabricated OLED devices were measured with Keithley 2635A SMU and Konica Minolta CS-100A, respectively. EL spectra and Commission Internationale de l'Eclairage (CIE) 1931 color coordinate were obtained using Konica Minolta CS-2000 spectroradiometer.

2. T_g , T_m , and T_d of synthesized materials from DSC and TGA measurement.

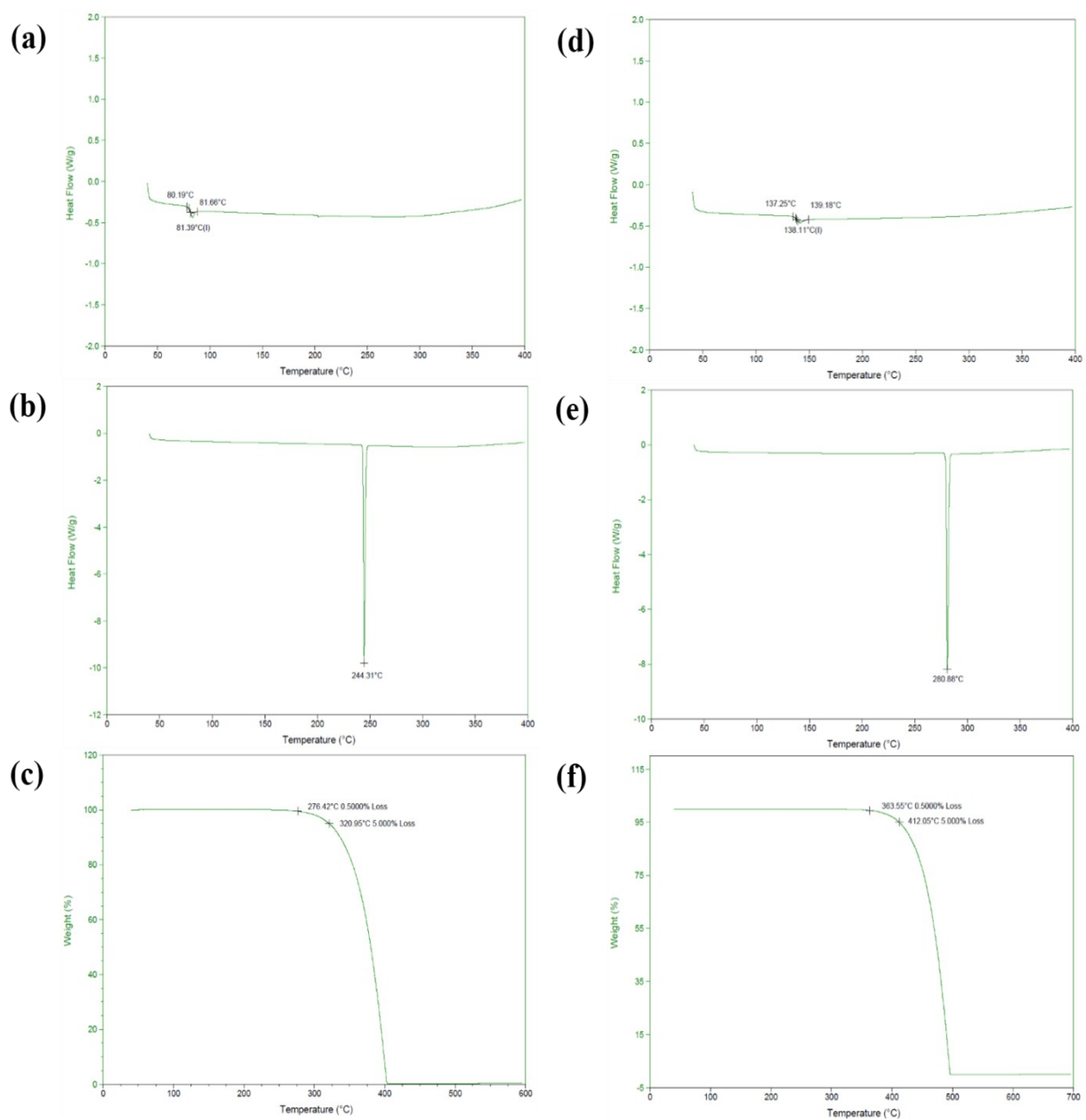


Figure S1. Differential scanning calorimetry (DSC) results of (a), (b) CzCbPy and (d), (e) 2CzCbPy and thermogravimetric analysis (TGA) results of (c) CzCbPy and (f) 2CzCbPy.

Table S1. Thermal properties of CzCbPy and 2CzCbPy

Hosts	T_g^a (°C)	T_m^b (°C)	T_d^c (°C)
CzCbPy	81	244	321
2CzCbPy	138	281	412

^{a)} Glass transition temperature and ^{b)} melting temperature scanned from DSC. ^{c)} Decomposition temperature measured by TGA at 5% weight loss.

3. Results of Cyclic Voltammetry.

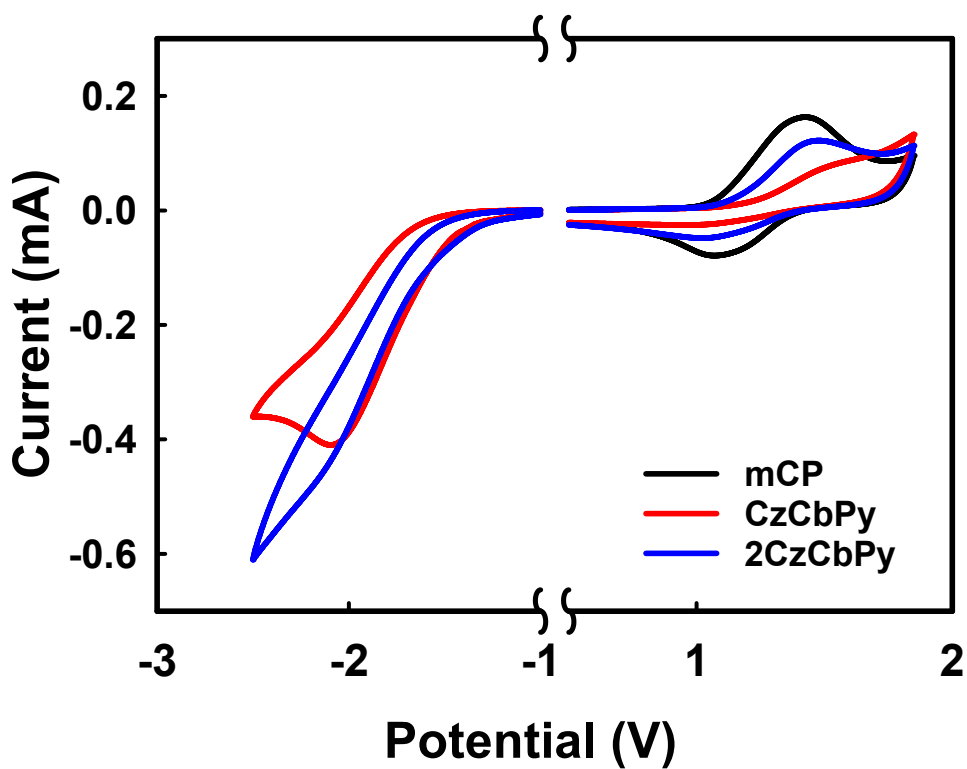


Figure S2. Cyclic voltammograms of mCP, CzCbPy, and 2CzCbPy.

4. Prompt and delayed PL spectra of DMAC-DPS in each host materials.

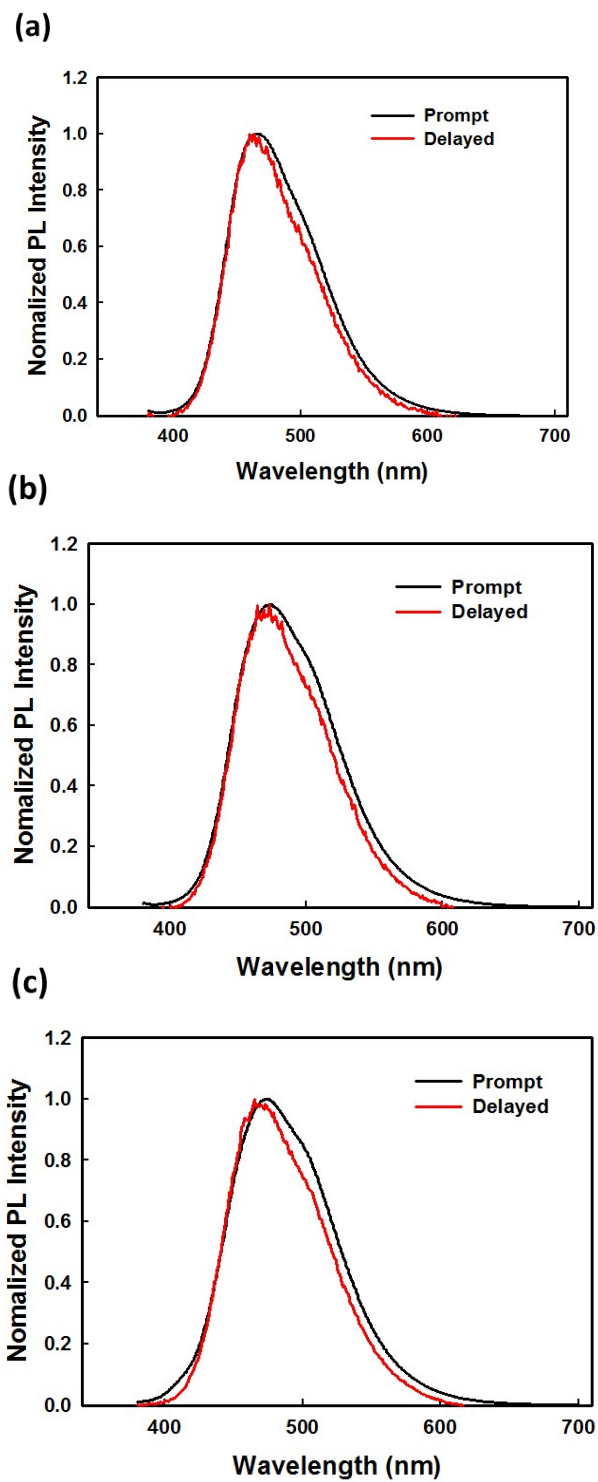


Figure S3. Prompt and delayed PL spectra of DMAC-DPS doped 20 wt% in (a) mCP, (b) CzCbPy and (c) 2CzCbPy.

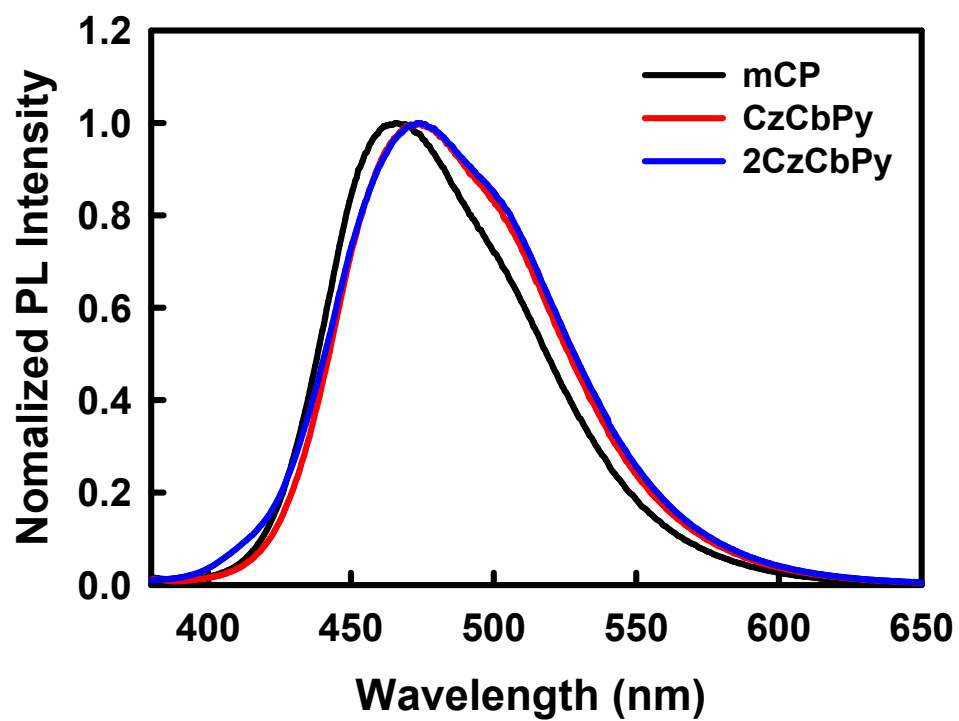


Figure S4. PL spectra of DMAC-DPS doped 20 wt% in mCP, CzCbPy and 2CzCbPy.

5. NMR data

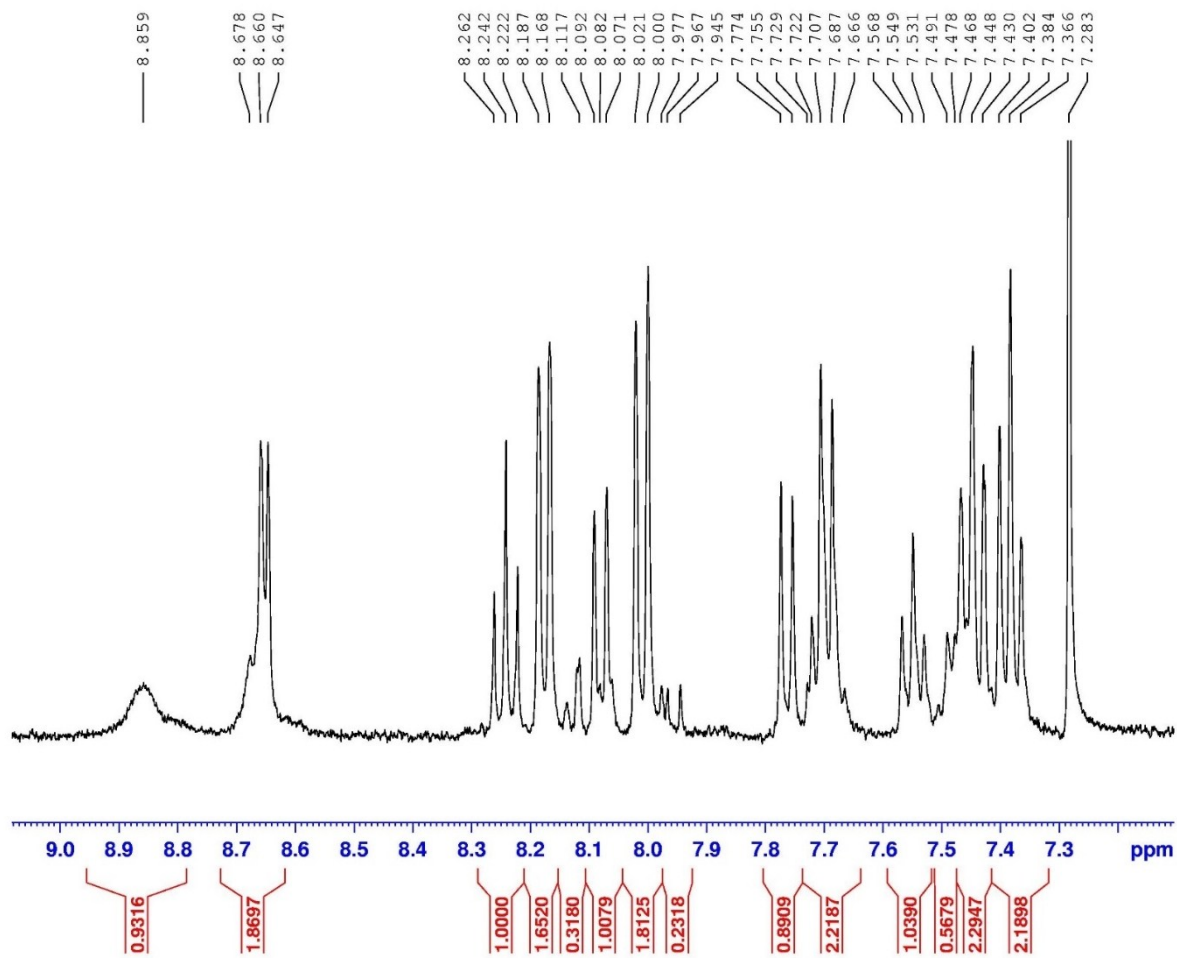


Figure S5. ^1H NMR spectrum of CzCbPy

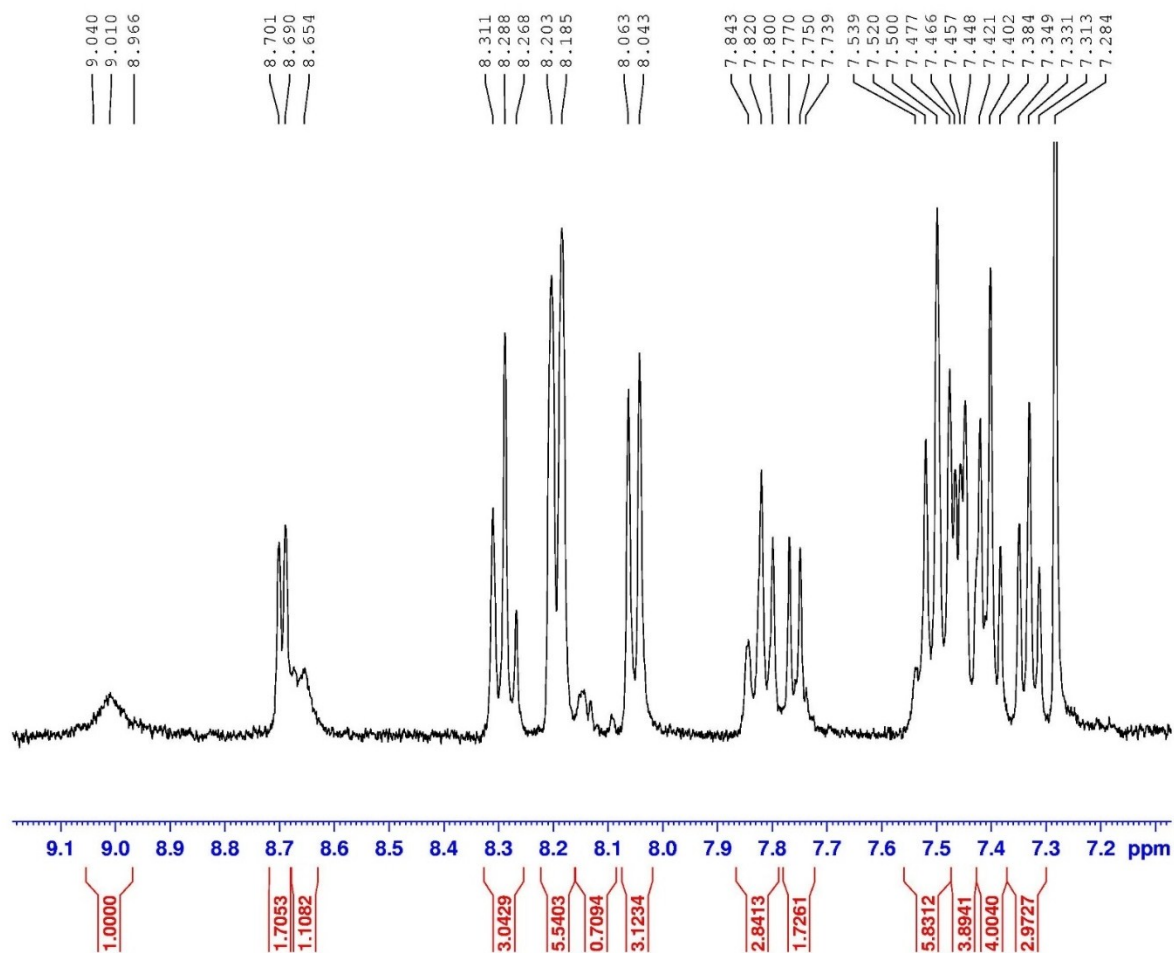


Figure S6. ^1H NMR spectrum of 2CzCbPy

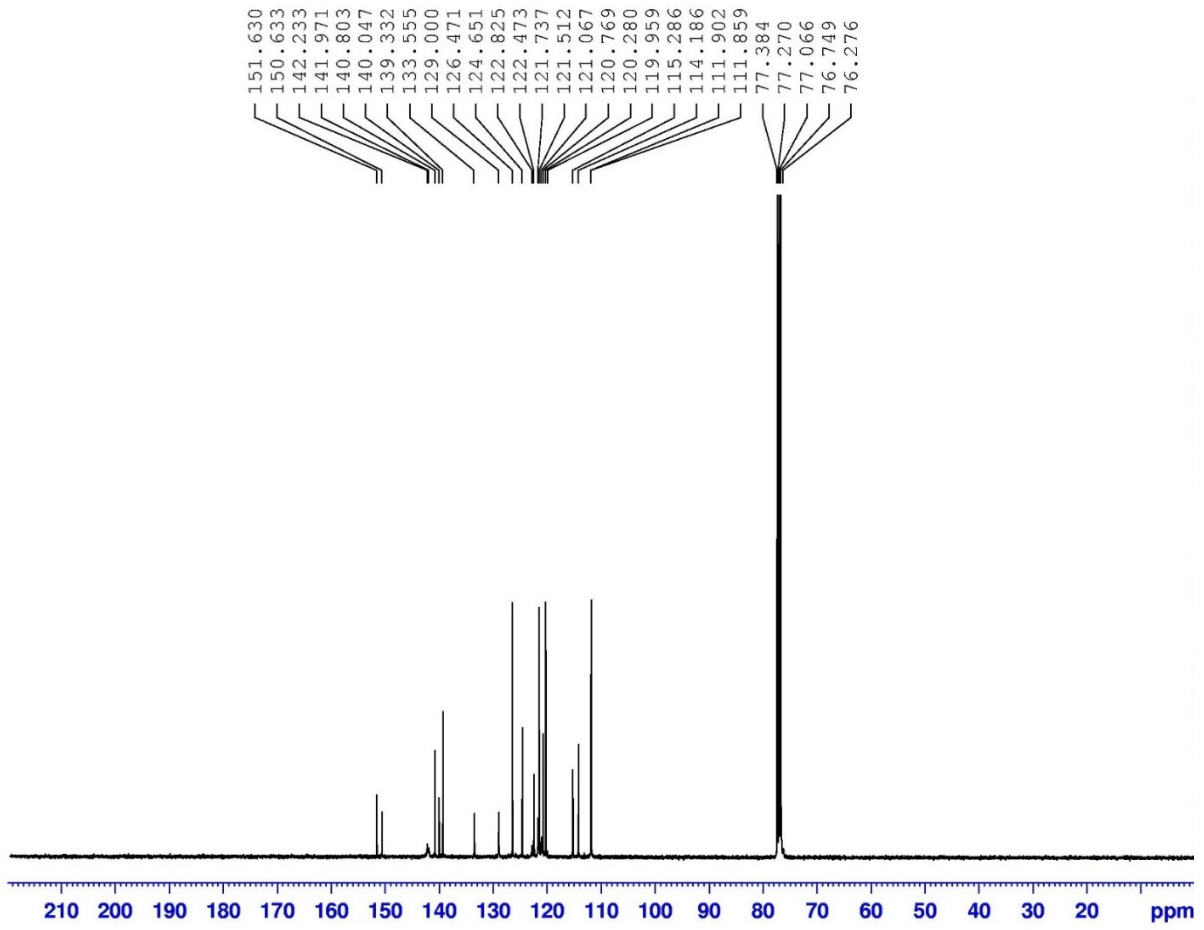


Figure S7. ¹³C NMR spectrum of CzCbPy

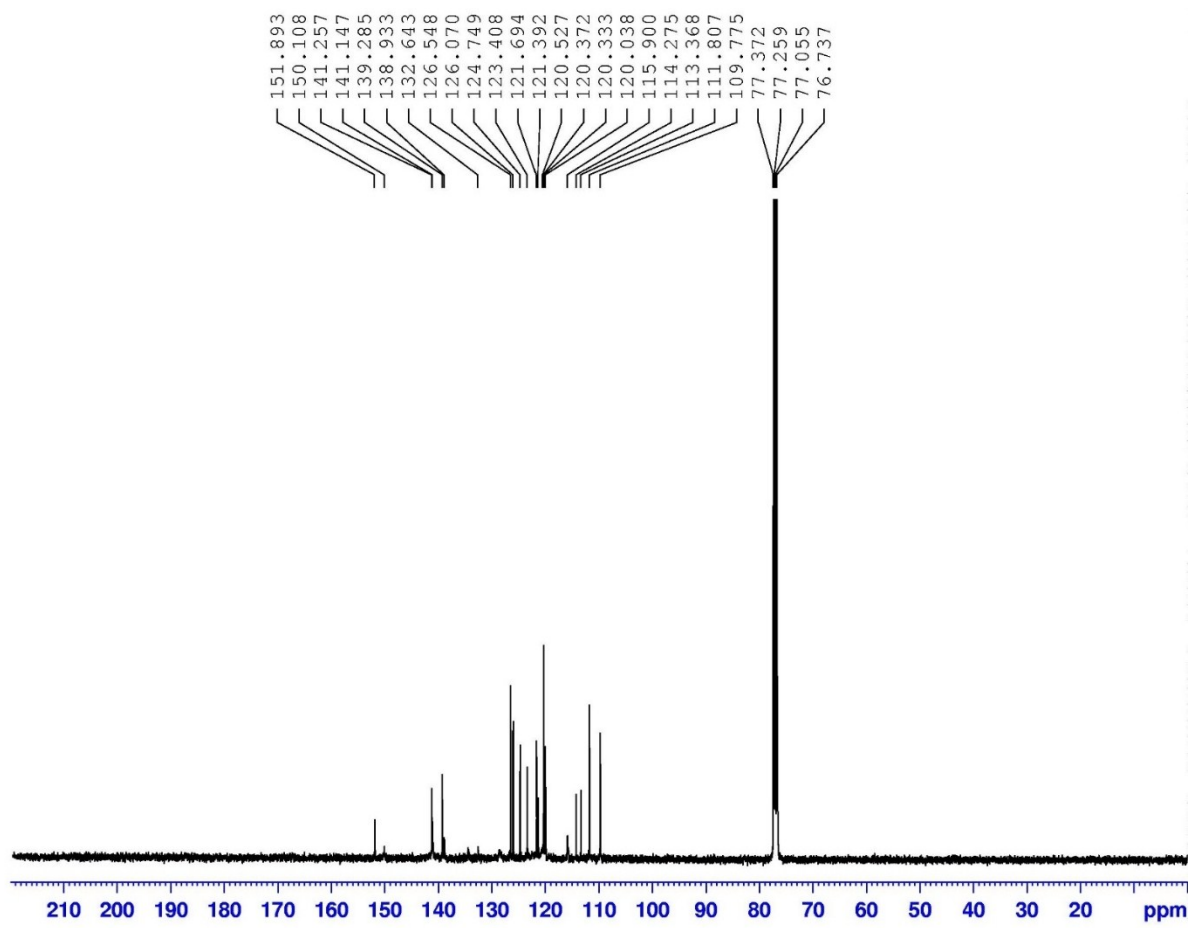


Figure S8. ^{13}C NMR spectrum of CzCbPy